Available online at www.sciencedirect.com
SCIENCE DIRECT®
International Journal of Pharmaceutics 314 (2006) 56–62
INTERNATIONAL JOURNAL OF PHARMACEUTICS
www.elsevier.com/locate/ijpharm

Pharmaceutical Nanotechnology

Structural investigations on nanoemulsions, solid lipid nanoparticles and nanostructured lipid carriers by cryo-field emission scanning electron microscopy and Raman spectroscopy

Anne Saupe [a,*], Keith C. Gordon [b], Thomas Rades [a]

[a] *School of Pharmacy, University of Otago, P.O. Box 56, Dunedin, New Zealand*
[b] *Department of Chemistry, University of Otago, P.O. Box 56, Dunedin, New Zealand*

Received 1 June 2005; received in revised form 13 December 2005; accepted 15 January 2006
Available online 30 March 2006

Abstract

Recently, colloidal dispersions based on solid lipids (solid lipid nanoparticles, SLN) and mixtures of solid and liquid lipids (nanostructured lipid carriers, NLC) were described as innovative carrier systems. A spherical particle shape is the basis of features such as a high loading capacity and controlled drug release characteristics due to smaller lipid–water interfaces and longer diffusion pathways when compared to thin platelets. The structures of SLN and the influence of oil load (NLC) on particle properties were investigated by photon correlation spectroscopy (PCS), laser diffractometry (LD), cryo-field emission scanning electron microscopy (cryo-FESEM), Raman spectroscopy and infrared spectroscopy (IR), and compared to a conventional nanoemulsion. PCS and LD data show similar size and size distribution for SLN and NLC (approximately 210 nm, polydispersity index approximately 0.15) and suggested a long term physical stability for the dispersions which had been stored for up to 12 months at different temperatures. Using cryo-FESEM droplets (for the nanoemulsion) and almost spherical particles for SLN and NLC were observed. Raman spectroscopy resulted in spectra for NLC that are weighted to the SLN spectra, suggesting an undisturbed crystal structure. Infrared spectra of the NLC are predominantly SLN in nature. Importantly the SLN bands are unshifted in the NLC spectrum indicating that the crystalline structure is unaffected by the presence of the oil.

Keywords: Solid lipid nanoparticles; Nanostructured lipid carriers; Cryo-FESEM; Raman spectroscopy

1. Introduction

Recently, solid lipid nanoparticles (SLN) (Muller et al., 2000; Mehnert and Mader, 2001) have been introduced to the literature as a carrier system for poorly water-soluble pharmaceutical drugs (Ugazio et al., 2002; Westesen et al., 1997) and cosmetic active ingredients (Lippacher et al., 2002, 2004; Jenning et al., 2000a; Wissing and Muller, 2003a,b). Advantages of SLN include a potentially wide application spectrum (dermal, oral, intravenous), the use of biodegradable physiological lipids or lipidic stabilisers which are generally recognized as save (GRAS) or have a regulatory accepted status, the production without organic solvents and the possibility of scaling up to industrial production level (Liedtke et al., 2000; Gohla and Dingler, 2001). SLN based on one lipid component however exhibit limited drug payloads and may result in potential drug expulsion from the crystal lattice due to polymorphic transitions of the lipid crystals or a reduction in their number of imperfections (Bunjes et al., 1996). To overcome this drawback, nanostructured lipid carriers (NLC) (Muller et al., 2002) have been developed based on a mixture of solid and liquid lipid (oil) which leads to an imperfect matrix structure. Liquid lipids usually show a higher solubility for drugs than solid lipids (Pouton, 2000). The aim of NLC-formulation is to create particles in which the oil is incorporated into the core of a solid lipid. This would lead to a higher loading capacity and controlled drug release as the drug is dissolved in the oil and simultaneously encapsulated in the solid lipid. Features such as the spherical shape of the particle and the entrapment of oil in the core of the particle may account for these properties (Jores et al., 2004; Muller et al., 2002). Different types of nanostructured lipid carriers are possible and discussed in the literature (Muller et al., 2002; Jores et

* Corresponding author. Tel.: +64 3 4797272; fax: +64 3 4797034.
E-mail address: anne.saupe@stonebow.otago.ac.nz (A. Saupe).

0378-5173/$ – see front matter © 2006 Elsevier B.V. All rights reserved.
doi:10.1016/j.ijpharm.2006.01.022

Table 1
Sample composition

Sample	% total lipid (w/w)	% CP (w/w)	% MCT (w/w)	% Tego Care 450 (w/w)
NE	10	0	10	1
SLN-dispersion	10	10	0	1
NLC-dispersion	10	9	1	1

al., 2004). Jores et al. (2004) found that high oil loads may lead to phase separation whereas Muller et al. (2002) and Jenning et al. (2000c) showed the formation of oily nanocompartments within the solid matrix. The aim of the present study was therefore to obtain experimental evidence of the microstructure of NLC, and to compare their physicochemical behaviour to nanoemulsions and SLN. Several analytical techniques, including photon correlation spectroscopy, laser diffractometry, cryo-FESEM, Raman and IR spectroscopy were applied to provide more detailed information on these nanoparticulate systems.

2. Materials and methods

Cetyl palmitate (CP) was a gift from Henkel (Germany). Miglyol® 812 (caprylic/capric triglycerides, MCT) was provided by Beiersdorf (Germany). Tego Care 450 (Polyglycerol-methylglucosedistearate) was donated by Goldschmidt (Germany). All other chemicals were obtained from Sigma (Germany).

2.1. Preparation of SLN-dispersion, NLC-dispersion and nanoemulsion

Table 1 gives an overview of the formulations investigated. For all formulations the hot lipid phase was dispersed in water, containing 1% Tego Care 450 as a surfactant at 75 °C and a premix was formed by homogenising in a high-speed stirrer (Ultra Turrax T25, Jahnke & Kunkel GmbH, Staufen, Germany) for 1 min at 8000 rpm. Nanodispersions were then prepared by a hot high pressure homogenisation technique using a Micron LAB 40 (APV Systems, Germany). Three cycles were carried out at 500 bar and 75 °C.

2.2. Particle size and zeta potential measurements

Laser diffractometry (LD) was carried out on a LS 230 instrument (Beckmann-Coulter Electronics, Germany). LD data were evaluated using the volume distribution, which means that, e.g. a diameter 90% (d90%) value of, e.g. 1 μm indicates that 90% of the particles possess a diameter of 1 μm or less. The values are calculated as the average of three measurements. Photon correlation spectroscopy (PCS) is used to determine the mean particle size (PCS diameter) and size distribution (polydispersity index, PI). PCS is a laser light scattering technique suitable for application to particles ranging in size from approximately 3 nm to 3 μm. PCS was performed using a Zetasizer 4 (Malvern Instruments, UK). The values were calculated as the average of 20 measurements. Zeta potentials (ZP) were also determined using the Zetasizer 4.

2.3. Cryo-field emission scanning electron microscopy (Cryo-FESEM)

A drop of dispersion was filled into brass rivets and plunge frozen in a liquid nitrogen slush. Samples were then stored in liquid nitrogen and transferred into the cryo stage (Gatan, Alto 2500, UK) of the microscope (JOEL, JSM-6700F, Japan). The sample was fractured on the cryo stage and coated with platinum. Images were acquired at a temperature at −140 °C and a voltage of 2.5 kV. All dispersions were investigated 30 days after preparation. Space bars are added into the figure to facilitate the estimation of the particles size.

2.4. Raman and infrared spectroscopy

FT-Raman spectra were collected using a Bruker IFS-55 interferometer with an FRA/106 S attachment. The excitation source was an Nd:YAG laser with an excitation wavelength of 1064 nm. A liquid nitrogen cooled Ge detector diode (D-418) was used to detect Raman photons. All spectra were taken with a laser power of 300 mW, over a 1 h period at a resolution of 4 cm^{-1}. Spectra were analysed using GRAMS 5.0 (Galactic Industries). ATR-IR spectra were recorded using a MIRacle Single reflection HATR accessory equipped with a zinc selenide crystal (Pike Technologies, Madison, WI, USA) on a Bruker Equinox 55 system. All spectra were collected using OPUS software. All dispersions were investigated 30 days after preparation.

3. Results

3.1. Effect of sample composition on particle size

Nanoparticle dispersions were prepared by high pressure homogenisation using a Micron LAB 40 (APV systems, Luebeck, Germany). The size of the particles depends on the production temperature, pressure and the number of homogenisation cycles (Liedtke et al., 2000). Beside production parameters, the nature of the lipid matrix, surfactant blend and viscosity of lipid and aqueous phase also influence the outcome. Leaving all the other parameters constant, in this study the only variable was the composition of the lipid matrix which has been changed from no oil load (SLN) to 10% medium chain triglycerides load (NLC) with respect to the lipid phase, and 100% MCT for the nanoemulsion (NE), respectively. All formulations were produced at 75 °C to ensure that the lipid remains in the liquid state during the production process.

Directly after hot high pressure homogenisation, all lipid formulations are nanoemulsions and should therefore form droplets

Table 2
Particle size of NE-formulation (top), SLN-formulation (middle) and NLC-formulation (bottom) determined by LD and PCS

Storage time	Storage temperature	LD: 50% of all particles smaller than (μm)	LD: 99% of all particles smaller than (μm)	PCS diameter (nm)	Polydispersity index
1 day		0.173	0.323	204	0.119
3 months	4 °C	0.142	0.358	202	0.165
	RT	0.131	0.349	205	0.153
	40 °C	0.198	0.395	209	0.169
6 months	4 °C	0.131	0.349	209	0.142
	RT	0.129	0.333	209	0.139
	40 °C	0.124	0.342	205	0.145
12 months	4 °C	0.149	0.335	211	0.145
	RT	0.133	0.366	208	0.158
	40 °C	0.158	0.379	209	0.124
1 day		0.138	0.333	202	0.139
3 months	4 °C	0.122	0.360	200	0.161
	RT	0.123	0.355	200	0.123
	40 °C	0.119	0.381	197	0.163
6 months	4 °C	0.122	0.323	211	0.122
	RT	0.122	0.314	201	0.137
	40 °C	0.119	0.332	203	0.099
12 months	4 °C	0.127	0.464	202	0.132
	RT	0.128	0.128	202	0.134
	40 °C	0.122	0.206	202	0.134
1 day		0.166	0.456	208	0.120
3 months	4 °C	0.164	0.536	213	0.133
	RT	0.132	0.461	213	0.141
	40 °C	0.130	0.477	217	0.146
6 months	4 °C	0.219	0.793	215	0.129
	RT	0.134	0.454	216	0.111
	40 °C	0.130	0.470	218	0.139
12 months	4 °C	0.136	0.441	215	0.130
	RT	0.133	0.439	215	0.132
	40 °C	0.127	0.422	215	0.132

Samples were stored for up to 12 months at different temperatures (4 °C, room temperature (25 °C, RT), 40 °C).

of similar size. The following crystallisation of cetyl palmitate (dropping point 46–51 °C) will however influence the size and shape of the nanoparticles in the SLN- and NLC-dispersion. The particle sizes obtained by static (LD) and dynamic light scattering (PCS) were in the same range and suggested the formulations remained in the nanometer range for the investigated period of 12 months (Table 2). Storage temperature had no influence on long term stability. The zeta potential of the NE was −48.0 mV, −53.0 for the SLN-formulation and −52.1 of the NLC-formulation, 1 day after production. Zeta potential values of >−30 mV indicate a high degree of physical stability. Differences in the results of the two sizing methods are not unexpected as they are based on different measurement principles. The presence of microparticles can be excluded for all samples. LD showed that more than 99% of the particles were smaller than 536 nm (d99%). Comparing the NE-, SLN- and NLC-formulations there is no dependence of the particle size on the oil load. LD and PCS measurements revealed basically similar particle sizes and size distribution with d50% of approximately 150 nm and d99% of approximately 400 nm.

3.2. Cryo-field emission scanning electron microscopy

The microstructure of the dispersions was investigated by electron microscopy studies. One advantage of using cryo-FESEM is that the liquid dispersion can be frozen and viewed in the frozen state. It is not necessary to separate the nanoparticles from the water matrix and thus the samples are investigated close to their natural state. The micrograph of the nanoemulsion demonstrated spherical droplets in the nanometer range (Fig. 1 top) which was in agreement with the size data determined by PCS. The SLN-dispersion had a different electron microscopic appearance, spherical but not perfectly round shaped particles were found (Fig. 1 middle). An oil load of 10% to the lipid matrix (NLC) did not change the morphology of the particles (Fig. 1 bottom). Also, perfectly spherical droplets suggestive of the presence of a separated MCT phase were not found in these samples, i.e. at a MCT load of 10% no phase separation was observed. Regarding size, cryo-FESEM demonstrated similar results to LD and PCS, with particle sizes of approximately 200–300 nm for all formulations.

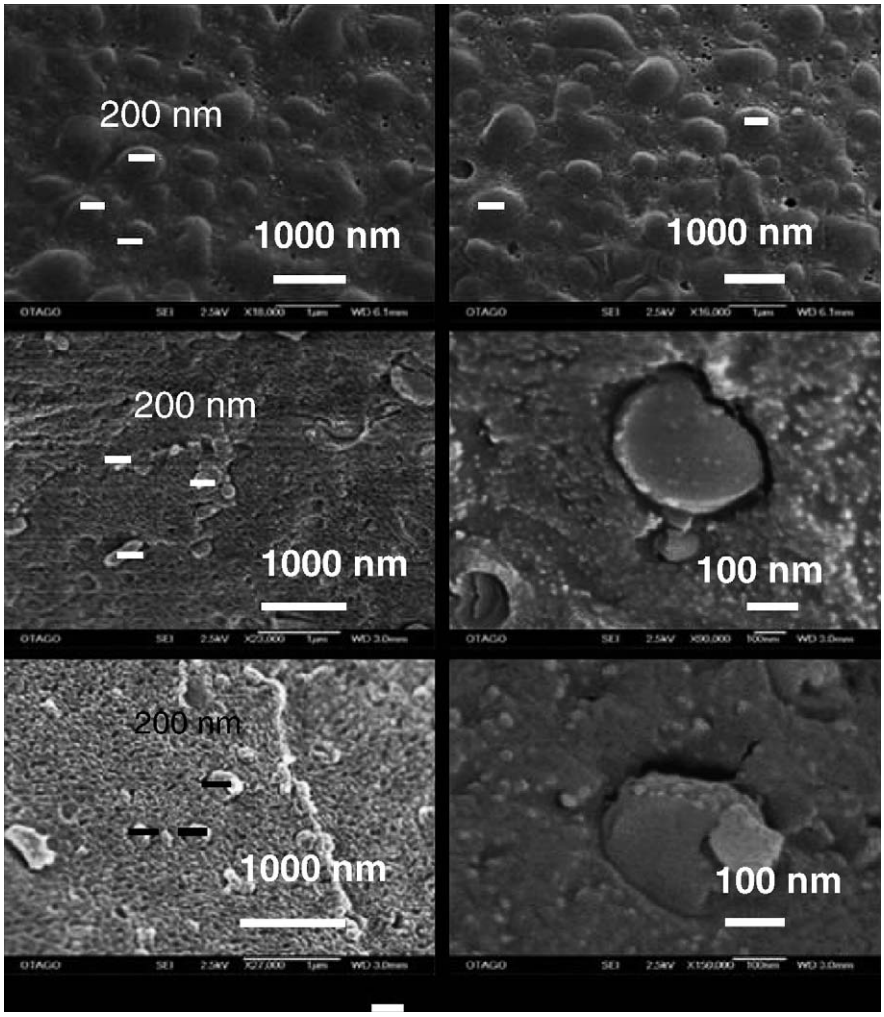

Fig. 1. Cryo-FESEM images of a colloidal formulations: NE (top), SLN (middle) and NLC (bottom).

The cryo-FESEM analysis revealed an almost spherical shape of the particles irrespective of the oil load of 10%. The most important result of the electron microscopic study is the absence of clearly identifiable oil droplets in the NLC samples. This is in contrast to the work of Jores et al. (2004) who found two-phase particles ("nanospoons") using cryo transmission electron microscopy. The lipid particles were described as platelet-shaped with the MCT separated from the solid lipid glycerol behenate, sticking on the surface of the particle. It appears that the use of different solid lipids (cetyl palmitate/glycerol behenate) can influence the shape and structure of the lipid particles.

3.3. Raman spectroscopy

Raman spectroscopy was used to obtain information about the structure and properties of molecules from their vibrational transitions (Andreev et al., 2001; Pratiwi et al., 2002; Tandon et al., 2000). Raman spectroscopy in this study is used to investigate the conformational order of hydrocarbon chains, i.e. if and how oil loading changes the lipid chain arrangement. It has been shown that Raman spectra of lipids are sensitive to conformational, packing and dynamical changes involving hydrocarbon chains (Jores, 2004; Wartewig and Neubert, 2005). Table 3 presents observed Raman bands and peak assignments according to the literature (Dollish et al., 1973).

The components used in this study (cetyl palmitate and MCT) have quite similar chemical structures. Cetyl palmitate is a wax produced by catalytic esterification of a fatty alcohol (cetylic alcohol) and a fatty acid (palmitic acid). MCT is a triglyceride mixture of capryl-, caprin- und lauric acid (fatty acids with a medium chain length). All components contain similar molecular moieties (e.g. CH_2, and ester groups) and differ mainly in the chain length of the fatty acids. The aim of the experiments was

Table 3
Observed Raman bands and peak assignments according to the literature (Dollish et al., 1973)

Band position (cm^{-1})	Assignment
Between 800 and 900	CH_3 rocking
1062	C–C asymmetric stretching
1128	C–C symmetric stretching
1294	CH_2 twisting
2845	CH_2 symmetric stretching
2881	CH_2 antisymmetric stretching

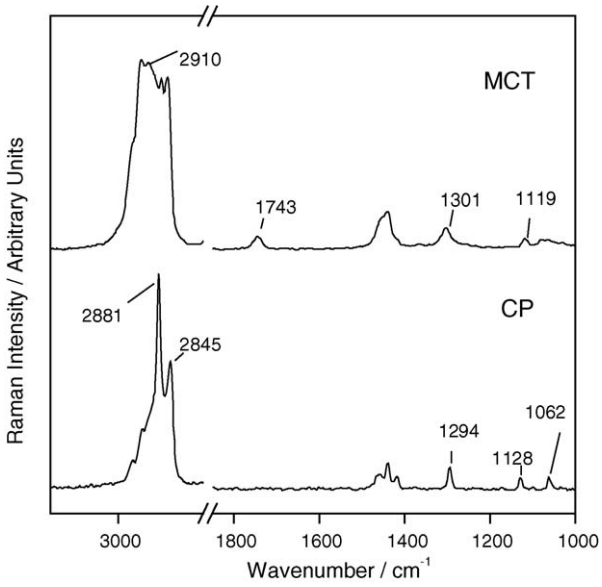

Fig. 2. Raman spectra of lipid components: MCT (upper spectrum), CP (lower spectrum).

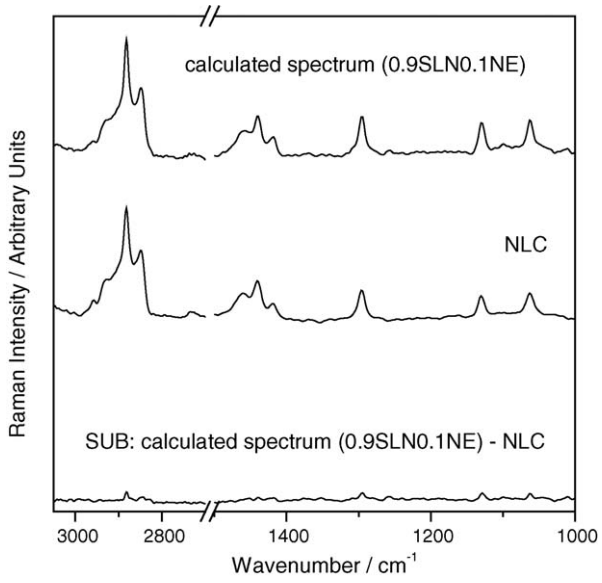

Fig. 4. Comparison of relative peak intensities of calculated spectrum (0.9 SLN, 0.1 NE) and NLC-formulation.

to investigate the application of Raman spectroscopy to the qualitative analysis of the aqueous NE-, SLN- and NLC-dispersions (Wartewig and Neubert, 2005). Raman spectroscopy is a particularly useful technique as it involves no sample preparation and most importantly allows measurements in the presence of water (Vankeirsbilck et al., 2002). Raman spectra were obtained from lipid components (CP, MCT) (Fig. 2) and all colloidal dispersions (Fig. 3). Of particular interest was the comparison of spectra of SLN- and NLC-formulations with a calculated addition spectrum of a mixture of SLN- and NE-formulation at a ratio of 9:1 (Fig. 4).

Fig. 2 shows spectra of MCT (upper spectrum) and cetyl palmitate (lower spectrum), following normalisation to the broad peak from 3500 to 3000 cm^{-1}. The Raman spectrum of MCT shows characteristic intense bands in the CH region at 2935, 2910, 2873 and 2855 cm^{-1} and weaker bands at 1743, 1301 and 1119 cm^{-1}. The cetyl palmitate spectra revealed strong bands at 2881 and 2845 cm^{-1}. Weaker bands are present at 1294, 1128 and 1062 cm^{-1}.

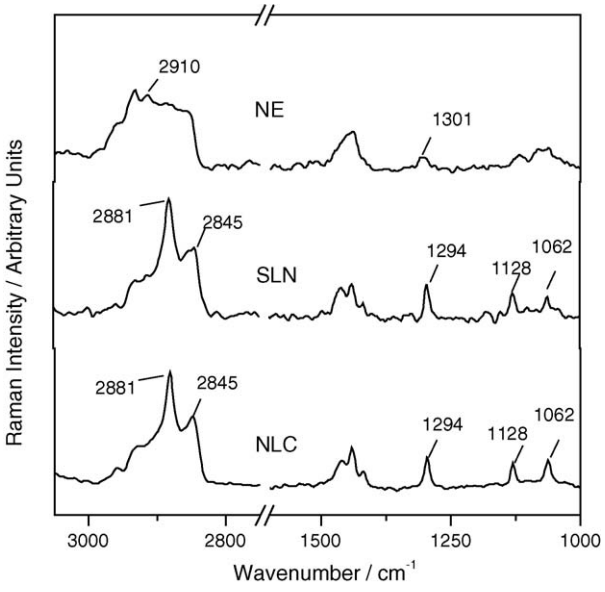

Fig. 3. Raman spectra of the nanoemulsion (NE)-, SLN- and NLC-formulation.

The Raman spectra of the NE-, SLN- and NLC-formulation are shown in Fig. 3. The spectra were again normalised to the peak ranging from 3500 to 3000 cm^{-1}. This peak is caused by water and is not shown in the figure. The characteristic peaks of the nanoemulsion were in agreement with those of MCT (Fig. 2). Both show bands at 2935, 2910, 2873, 2855 and 1743 cm^{-1}. The same was observed for the SLN-formulation and cetyl palmitate. The characteristic peaks at 2882, 2845, 1294, 1128 and 1062 cm^{-1} were visible in both spectra. For the NLC spectra the characteristic cetyl palmitate peaks at 2881, 2845, 1294, 1128 and 1062 cm^{-1} were observed. A typical MCT peak at 2935 cm^{-1} was found, but the characteristic MCT peak at 1743 cm^{-1} was not detectable. A typical MCT peak at 1301 cm^{-1} was only found in the NE-formulation suggesting the absence of free MCT in all other samples. A cetyl palmitate peak at 2881 cm^{-1} was found in all spectra except in MCT and NE spectra, indicating the presence of solid lipid. The Raman spectrum of the nanoemulsion is characterised by random coiled chains, while those of SLN- and NLC-formulations clearly show sharp bands at 1128 and 1062 cm^{-1} indicating the high conformational order of the acyl chains. The symmetric stretching of the methylene groups (peak at 2881 cm^{-1}) indicates the high degree of chain order in the SLN- and NLC-formulation. In contrast, the signal at 2881 cm^{-1} in the spectrum of the NE-formulation is much weaker. The appearance of the sharp stretching bands at 1062, 1128 and 2845 in the SLN- and NLC-formulation demonstrates that the acyl chains are well ordered.

Differences between the various formulations were also observed between 2930 and 2840 cm^{-1} (Fig. 3).

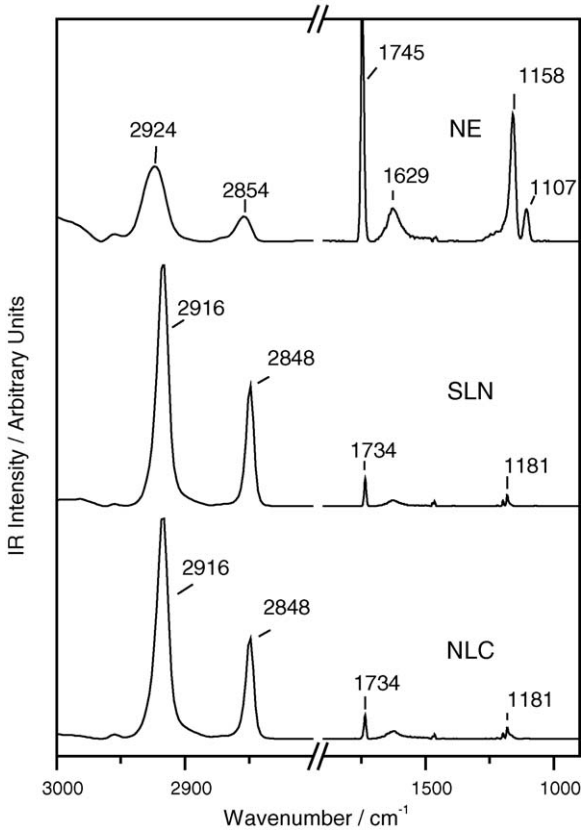

Fig. 5. Infrared spectra of the nanoemulsion (NE)-, SLN- and NLC-formulation.

It has been shown that nanoemulsions are weaker scatterer than the solid dispersion SLN, the peak maxima at 3223 cm^{-1} was seven times lower for the nanoemulsion than for the SLN-dispersion.

To determine whether the NLC-formulation spectrum is a simple mixture of spectra of nine parts SLN-formulation and one part nanoemulsion, a spectrum was calculated as a linear combination of 0.9 times the pure SLN spectrum plus 0.1 times the pure nanoemulsion spectrum. This calculated spectrum was compared to the NLC spectrum (Fig. 4). Main peak positions did not change. Sharp bands at 2881, 2845, 1294, 1128 and 1062 cm^{-1} are visible in both, the NLC and the calculated spectra. Subtraction of the normalised spectra led to a basically flat line indicating no major differences between the experimental and calculated spectra; suggesting that there are no major interactions between the molecules of the solid lipid and the liquid lipid oil.

However, it was noted that NLC are a weaker scatterer than the solid dispersion SLN. The peak maxima at 2881 cm^{-1} for the NLC was 10 times lower than what would be expected if the calculated spectra would be a simple combination of 0.9 times the pure SLN spectrum plus 0.1 times the pure nanoemulsion spectrum. As mentioned above, also nanoemulsions are weaker scatterer than the solid dispersion SLN.

In order to examine this finding further the respective IR spectra were measured. Using ATR in which the penetration depth exceeds 1 μm and thus all of the nanoparticles will be sampled we find that the spectrum is dominated by the SLN signature. The bands are unshifted from pure SLN and this strongly suggests that the SLN in the NLC particles is completely unperturbed by the addition of the oil (bands at 2916, 2848, 1734 and 1181 cm^{-1}). However bands in the nanoemulsion spectrum can be found at 2924, 2854, 1745, 1629 and 1158 cm^{-1} (Fig. 5). Such a finding is consistent with a system in which the oil does not intimately disturb the crystalline layer.

4. Discussion

In the present study three different nanoparticulate systems with a similar particle size of approximately 200 nm and long term physical stability were investigated. Differences in the microstructure were shown using cryo-FESEM and IR- and Raman spectroscopy. Nanoemulsions and solid lipid nanoparticles are well characterised systems; however the mixture of solid and liquid lipid does not appear to result in the formation of homogenous particles. Those described in the literature are either a structure consisting of oily nanocompartments in a solid (crystalline) particle (Jenning et al., 2000b,c; Muller et al., 2002) or a structure in which the solid lipid remains in an amorphous state "structureless type" after high pressure homogenisation (Muller et al., 2002). On the other hand, NLC also were described as platelet-shaped particles with separated MCT sticking on the surface. NLC with higher amounts of MCT were called "nanospoons" described as SLN platelets with sticking MCT droplets on the surface (Jores et al., 2004).

Electron microscopy of NLC-dispersions in this study indicates that the components are not completely separated as separated oil droplets were not visible in the electron micrographs of the NLC-dispersion. DSC investigations on these systems clearly demonstrated the absence of a supercooled melt, i.e. the presence of an amorphous state of the lipid (Saupe et al., 2005). Cryo-FESEM, IR and DSC data indicate that the NLC are predominantly crystalline. The qualitative interpretation of the Raman and infrared spectra reveal that oil presence did not lead to a change in lipid chain arrangement of the solid lipid cetyl palmitate. Because of the colloidal size of the particles, the Raman signal essentially comes from the complete particle. Assuming this, it appears most likely that the MCT is indeed in spacial separation from the crystalline part of the particles. The finding that the overall scattering pattern of the NLC was much lower than expected from a linear combination of nine parts SLN and one part NE dispersion does not describe a model for NLC as a physical mixture of SLN and NE. However, whether the oil is incorporated within the particles, or as a coat at the outside requires further investigation.

Acknowledgements

All formulations were produced at the Department of Pharmaceutical Technology at the Free University of Berlin. Also, the particle size and zeta potential measurements were carried out in Berlin. The support of Prof. R.H. Müller is gratefully acknowledged.

References

Andreev, G., Schrader, B., Schulz, H., Fuchs, R., Popov, S., Handjieva, N., 2001. Fresen. J. Anal. Chem. 371, 1009–1017.

Bunjes, H., Westesen, K., Koch, M.H.J., 1996. Int. J. Pharm. 129, 159–173.

Dollish F.R., Fateley W., Bentley F., 1973. Charecteristic Roman Frequencies of Organic Compounds, Wiley-Interscience, New York.

Gohla, S.H., Dingler, A., 2001. Die Pharmazie 56, 61–63.

Jenning, V., Gysler, A., Schafer-Korting, M., Gohla, S.H., 2000a. Eur. J. Pharm. Biopharm. 49, 211–218.

Jenning, V., Mader, K., Gohla, S.H., 2000b. Int. J. Pharm. 205, 15–21.

Jenning, V., Thunemann, A.F., Gohla, S.H., 2000c. Int. J. Pharm. 199, 167–177.

Jores, K., 2004. Lipid nanodispersions as drug carrier systems – a physicochemical characterization. Ph.D. Thesis. Martin-Luther-Universität Halle-Wittenberg.

Jores, K., Mehnert, W., Drechsler, M., Bunjes, H., Johann, C., Mader, K., 2004. J. Control. Release 95, 217–227.

Liedtke, S., Wissing, S., Muller, R.H., Mader, K., 2000. Int. J. Pharm. 196, 183–185.

Lippacher, A., Muller, R.H., Mader, K., 2002. Eur. J. Pharm. Biopharm. 53, 155–160.

Lippacher, A., Muller, R.H., Mader, K., 2004. Eur. J. Pharm. Biopharm. 58, 561–567.

Mehnert, W., Mader, K., 2001. Adv. Drug Deliv. Rev. 47, 165–196.

Muller, R.H., Mader, K., Gohla, S., 2000. Eur. J. Pharm. Biopharm. 50, 161–177.

Muller, R.H., Radtke, M., Wissing, S.A., 2002. Int. J. Pharm. 242, 121–128.

Pouton, C.W., 2000. Eur. J. Pharm. Sci. 11, S93–S98.

Pratiwi, D., Fawcett, J.P., Gordon, K.C., Rades, T., 2002. Eur. J. Pharm. Biopharm. 54, 337–341.

Saupe, A., Wissing, S.A., Lenk, A., Schmidt, C., Muller, R.H., 2005. Biomed. Mater. Eng. 15, 393–402.

Tandon, P., Forster, G., Neubert, R., Wartewig, S., 2000. J. Mol. Struct. 524, 201–215.

Ugazio, E., Cavalli, R., Gasco, M.R., 2002. Int. J. Pharm. 241, 341–344.

Vankeirsbilck, T., Vercauteren, A., Baeyens, W., Van der Weken, G., Verpoort, F., Vergote, G., Remon, J.P., 2002. TRAC Trends Anal. Chem. 21, 869–877.

Wartewig, S., Neubert, R.H.H., 2005. Adv. Drug Deliv. Rev. 57, 1144–1170.

Westesen, K., Bunjes, H., Koch, M.H.J., 1997. J. Control. Release 48, 223–236.

Wissing, S.A., Muller, R.H., 2003a. Int. J. Pharm. 254, 65–68.

Wissing, S.A., Muller, R.H., 2003b. Eur. J. Pharm. Biopharm. 56, 67–72.